

Charge Kondo anomalies in PbTe doped with Tl impurities

T. A. Costi¹ and V. Zlatić^{1,2,3}

¹*Peter Grünberg Institut and Institute for Advanced Simulation,
Forschungszentrum Jülich, D-52425 Jülich, Germany*

²*Institute of Physics, HR-10001 Zagreb, Croatia*

³*J. Stefan Institute, SI-1000 Ljubljana, Slovenia*

(Dated: January 19, 2012)

We investigate the properties of PbTe doped with a small concentration x of Tl impurities acting as acceptors and described by Anderson impurities with negative onsite correlation energy. We use the numerical renormalization group method to show that the resulting charge Kondo effect naturally accounts for the unusual low temperature and doping dependence of normal state properties, including the self-compensation effect in the carrier density and the nonmagnetic Kondo anomaly in the resistivity. These are found to be in good qualitative agreement with experiment. Our results for the Tl s -electron spectral function provide a new interpretation of point contact data.

PACS numbers: 71.27.+a, 72.10.Fk, 72.15.Qm

Introduction.— PbTe is a narrow gap semiconductor with a band gap of 190 meV at zero temperature [1]. Upon doping with Tl impurities [1, 2] a number of striking anomalies appear in the low temperature properties. These anomalies, described below, are currently not well understood. They are believed to be due to the special nature of Tl impurities in PbTe, which have been proposed to act as negative U centers, where $U < 0$ is an attractive onsite Coulomb energy. In compounds, the outer 6s shell of Tl can be empty, singly occupied or doubly occupied. A negative Coulomb correlation results in the nonmagnetic empty and doubly occupied states being lower in energy than the magnetic singly occupied state. Hybridization of the s -states with the valence band states of PbTe can then result, via dynamic valence fluctuations, in a (nonmagnetic) charge Kondo (CK) analogue [3, 4] of the conventional spin Kondo effect [5]. This nonmagnetic CK effect has been argued to explain many of the observed properties of $\text{Pb}_{1-x}\text{Tl}_x\text{Te}$ [6–10] which would then constitute the first physical realization of this effect.

A remarkable feature of $\text{Pb}_{1-x}\text{Tl}_x\text{Te}$ is that the low temperature properties depend sensitively on the Tl concentration, with a qualitatively different behavior below and above a critical concentration $x_c \simeq 0.3$ % Tl. For example, while $\text{Pb}_{1-x}\text{Tl}_x\text{Te}$ remains metalliclike down to the lowest temperatures for $x < x_c$, for $x > x_c$ it becomes superconducting with a transition temperature $T_c(x)$ increasing linearly with x and reaching 1.5 K at $x = 1.5$ % Tl [6, 11]. This is surprisingly high given the low carrier density of less than 10^{20} holes/cm³. In addition, measurements of the Hall number $p_H = 1/R_{He}$ [8, 12] indicate that the number of holes grows linearly with x for $x < x_c$, whereas for $x > x_c$ the number of holes remains almost constant: the system exhibits “self-compensation” and the chemical potential is pinned to a value $\mu = \mu^* \simeq 220$ meV [12, 13]. Transport measurements also show anomalous behavior at low tempera-

tures: while for $x < x_c$, the residual resistivity, ρ_0 , is very small and almost constant as a function of x , for $x > x_c$, ρ_0 increases linearly with x [9]. For $x < x_c$, the resistivity, $\rho(T)$, exhibits a positive slope at low temperature, while for $x > x_c$, the slope is negative and a Kondo-like contribution, $\rho_{imp}(T)$, is observed for $T \lesssim 10$ K [6, 9]. The origin of this anomaly is not due to magnetic impurities, since the susceptibility is diamagnetic [6].

In this Letter, we show that the unusual concentration and low temperature dependence of a number of normal state properties of $\text{Pb}_{1-x}\text{Tl}_x\text{Te}$ can be naturally explained within a picture of dilute Tl impurities acting as negative U centers in the PbTe host. Such a dilute impurity description is suggested by the observed concentration dependence of many properties, as summarized above, e.g., the linear dependence on x of the residual resistivity for $x > x_c$. We model the Tl impurities by the negative U Anderson model [14] and solve this for the static and dynamic properties by using the numerical renormalization group (NRG) method [15]. Our results, with comparisons to experimental data, and previous experimental and theoretical work on $\text{Pb}_{1-x}\text{Tl}_x\text{Te}$ [6, 7, 16], provide strong evidence that the CK effect [3] is realized in this system.

The idea that doping PbTe with Tl induces resonant states in the valence band of PbTe was conjectured early on (see Ref. 1). These states are mainly of Tl s -character and lie close to the top of the valence band, as recently shown by density functional theory calculations [17]. Resonant states alone, however, and generalizations of this to an impurity band of resonant states, cannot explain properties such as the superconductivity of $\text{Pb}_{1-x}\text{Tl}_x\text{Te}$. For this, a coupling of Tl ions to the lattice [18], or a static mixed valence model [19] have been proposed. In the latter, Tl impurities, known to be valence skippers in compounds, are assumed to dissociate into energetically close Tl^{1+} ($6s^2p^1$) and Tl^{3+} ($6s^0p^3$) ions, while the Tl^{2+} ($6s^1p^2$) configuration lies higher in energy

[20]. In the highly polarizable PbTe host, this can result in negative on-site U and provides a mechanism for superconductivity and a qualitative explanation for the observed self-compensation, chemical potential pinning and the diamagnetic behavior of $\text{Pb}_{1-x}\text{Tl}_x\text{Te}$ [19]. For a more quantitative explanation of the observed anomalies, and in order to explain the Kondo anomalies in the resistivity, a more realistic model is needed, which includes dynamic fluctuations between the Tl^{1+} and Tl^{3+} valence states. This motivates our use of the negative U Anderson model [14], as formulated for $\text{Pb}_{1-x}\text{Tl}_x\text{Te}$ in Ref. 7 and discussed as a model for this system in Refs. 6–10, 16, 21. For completeness, we mention also the valence band model for PbTe, in which the main effect of Tl doping is assumed to be a rigid shift of the chemical potential into the valence band. This model may be relevant for the transport properties of PbTe doped with Tl impurities [22] at high temperature ($T > 300\text{K}$), where the charge Kondo effect is suppressed. It fails, however, to describe the low temperature anomalies that we are addressing in this Letter, e.g. the Kondo upturn in the resistivity at $T < 10\text{K}$ for $x > x_c$.

Model and calculations.— We consider n Tl impurities in a PbTe crystal with N Pb sites described by the Hamiltonian $H = H_{\text{band}} + H_{\text{imp}} + H_{\text{hyb}}$. The first term, $H_{\text{band}} = \sum_{\mathbf{k}\sigma} (\epsilon_{\mathbf{k}} - \mu_e) c_{\mathbf{k}\sigma}^\dagger c_{\mathbf{k}\sigma}$, describes the valence p -band of PbTe, where μ_e is the (electron) chemical potential and $c_{\mathbf{k}\sigma}^\dagger$ creates an electron with energy $\epsilon_{\mathbf{k}}$. The second term, $H_{\text{imp}} = (\epsilon_0 - \mu_e) \sum_{i=1}^n \hat{n}_{i\sigma} + U \sum_{i=1}^n n_{i\uparrow} n_{i\downarrow}$, describes the Tl impurities, where $n_{i\sigma} = s_{i\sigma}^\dagger s_{i\sigma}$ is the number operator for a Tl s -electron at site i with spin σ and energy ϵ_0 , and U is the (negative) correlation energy. The last term, $H_{\text{hyb}} = \sum_{i=1}^n \sum_{\mathbf{k}\sigma} V_0 (c_{\mathbf{k}\sigma}^\dagger s_{i\sigma} + h.c.)$, models the hybridization of Tl s -states with the valence band p -states and V_0 is the matrix element for the s - p interaction. Its strength is characterized by the hybridization function $\Delta(\omega) = \pi V_0^2 \sum_{\mathbf{k}} \delta(\omega - \epsilon_{\mathbf{k}\sigma}) = \pi V_0^2 \mathcal{N}(\omega)$, where we retain the full energy dependence of the p -band density of states $\mathcal{N}(\omega) = \sum_{\mathbf{k}} \delta(\omega - \epsilon_{\mathbf{k}})$ of PbTe [22].

The chemical potential μ_e determines $n_e = \frac{1}{N} \sum_{\mathbf{k}\sigma} \langle c_{\mathbf{k}\sigma}^\dagger c_{\mathbf{k}\sigma} \rangle$ and $n_s = \frac{1}{n} \sum_{i=1}^n \sum_{\sigma} \langle n_{i\sigma} \rangle$, the average number of p and s electrons per site. We denote by $x = n/N$ the concentration of Tl impurities. Since Tl acts as an acceptor, the ground state corresponds to the Tl^{1+} ($n_s = 2$) configuration and the Tl^{3+} ($n_s = 0$) configuration is split-off from the ground state by the energy $\delta = E(\text{Tl}^{3+}) - E(\text{Tl}^{1+}) > 0$. A concentration x of Tl impurities accommodates $x(n_s - 1)$ electrons (per Tl site), where the number of accepted electrons in the $6s$ level of Tl is measured relative to the neutral Tl^{2+} (s^1) configuration having $n_s = 1$. These electrons are removed from the valence band leaving behind $n_0 = 1 - n_e$ holes. Thus, charge neutrality implies $n_0 = x(n_s - 1)$ [7], which for a given x and temperature T has to be satisfied by adjusting the chemical potential μ_e . Here, we neglect in-

terimpurity interactions and solve H for a collection of single independent negative- U centers by using the NRG [15]. For each x and each T we satisfy the above equation by self-consistently determining the chemical potential μ_e (or equivalently the hole chemical potential μ , which we henceforth use).

The electrical resistivity of electrons scattering from a dilute concentration x of Tl impurities is obtained from the usual expression, $\rho_{\text{imp}}(T) = 1/e^2 L_{11}$, where L_{11} is the static limit of the current-current correlation function. In the absence of nonresonant scattering the vertex corrections vanish and the relevant transport integral L_{11} can be written as [23],

$$L_{11} = \sigma_0 \int_{-\infty}^{\infty} d\omega \left(-\frac{\partial f(\omega)}{\partial \omega} \right) \mathcal{N}(\omega) \tau(\omega, T), \quad (1)$$

where $\sigma_0 = \langle v_{\mathbf{k}_F}^2 \rangle$ is the velocity factor v_k^2 averaged over the Fermi surface, $f(\omega) = 1/[1 + \exp(\omega/k_B T)]$ is the Fermi function, $\tau(\omega, T)$ is the conduction-electron transport time [23] $\tau(\omega, T)^{-1} = 2n_{\text{Tl}} V_0^2 A(\omega, T)$ and $A(\omega, T) = -\frac{1}{\pi} \text{Im} G(\omega + i0^+)$ is the spectral function of s -electrons. The number of Tl impurities n_{Tl} per cm^3 is related to x in percent by $n_{\text{Tl}} = 1.48 \times 10^{20} x$ [24].

Choice of model parameters.— We use $\mu^* \approx 225\text{ meV}$, close to the value obtained from tunneling experiments [12, 13]. Other parameters, such as $\Delta_0 = \Delta(\mu^*)$, required to fix the hybridization function $\Delta(\omega)$, and U are largely unknown. Our interpretation of the tunneling spectra (see discussion of Fig. 2 below), suggests $U \approx -30\text{ meV}$. The measured Kondo-like resistivity for $x \geq x_c$ at low temperatures requires that $|U| \gg \Delta_0$. We take $U/\Delta_0 = -11$ with $\Delta_0 = 2.7\text{ meV}$ to yield a Kondo temperature $T_K \approx 1.23\text{ K}$ below the highest $T_c \approx 1.5\text{ K}$ at $x = 1.5\%$ $\gg x_c$, where T_K is defined via the impurity resistivity $\rho_{\text{imp}}(T = T_K) = 0.5\rho_{\text{imp}}(T = 0)$ for $x \gg x_c$. The overall qualitative aspects of our results remained the same for values of U in the range $10\text{ meV} \leq |U| \leq 220\text{ meV}$ and $|U|/\Delta_0 \gg 1$.

Qualitative considerations.— It is instructive to first make some qualitative remarks, starting from the atomic limit $V_0 = 0$ [7]. For $x = 0$ the chemical potential lies in the gap between the valence and conduction bands. For finite but very small x each Tl impurity accepts one electron, i.e. $n_s \approx 2$ and $n_0 = x(n_s - 1) \approx x$ grows linearly with x . At the same time, the chemical potential shifts downwards into the valence band $\mu < E_v$, where E_v denotes the top of the valence band. This implies that the splitting $\delta(\mu) = -(2(\epsilon_0 - \mu) + U)$ between donor and acceptor configurations decreases. Eventually, at a critical concentration $x = x^*$, the chemical potential reaches $\mu = \mu^* = \epsilon_0 + U/2$ where $\delta(\mu) = 2(\mu - \mu^*) = 0$ and the system is in a (static) mixed valence state where the Tl^{1+} and Tl^{3+} configurations are degenerate. In this situation $n_s = 1$, and further doping cannot increase the hole carrier density beyond the value $n_0(\mu^*)$, i.e. one has

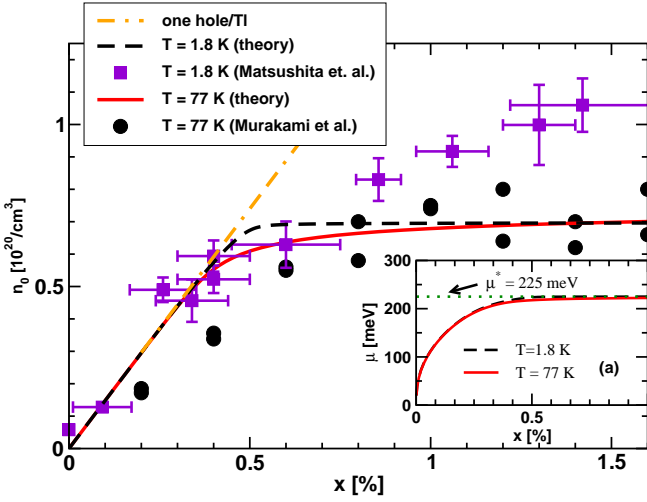


FIG. 1: (Color online) Hole carrier density n_0 versus Tl doping x in % for $T = 1.8$ K and $T = 77$ K. Filled circles: experimental data at $T = 77$ K [12], filled squares: experimental data at $T = 1.8$ K [8], dot-dashed line: expected n_0 for one hole per Tl. Inset (a): hole chemical potential μ versus x at $T = 1.8$ K and $T = 77$ K [and hence $\delta(\mu) = 2(\mu - \mu^*)$].

self-compensation with a pinning of the chemical potential to μ^* [7].

For finite V_0 , quantum fluctuations between the degenerate states Tl^{1+} and Tl^{3+} at $\mu = \mu^*$ become important and lead to a CK effect. This significantly affects all static and dynamic properties and needs to be taken into account in describing the experiments. It is also important for $\mu > \mu^*$, since a finite charge splitting $\delta(\mu) > 0$ in the negative- U Anderson model is similar to a Zeeman splitting in the conventional spin Kondo effect [25]. The latter is known to drastically influence all properties [5]. Thus, for the whole range of concentrations x , one expects fluctuations to play an important role in the properties of $\text{Pb}_{1-x}\text{Tl}_x\text{Te}$.

Numerical results.— Figure 1 shows $n_0(x)$ versus x at $T = 1.8$ K and at $T = 77$ K and a comparison with experimental data on Hall number measurements [8, 12]. At low dopings, n_0 is linear in x both in theory and in experiment, as expected for Tl impurities acting as acceptors (dot-dashed curve in Fig. 1). However, the efficiency, $n_0(x)/n_{\text{Tl}}(x)$, of Tl dopants in supplying holes at low x is only around 65 % in the data of Ref. 12 as opposed to 100 % in our model calculations and in the data of Ref. 8. At higher dopings $n_0(x)$ saturates rapidly with increasing x for $T = 1.8$ K and more slowly at higher temperatures. The theoretical crossover from linear to saturated behavior occurs at $x = x^* \approx 0.5$ %, larger than the value $x_c \approx 0.3$ % for the onset of superconductivity. The theoretical saturation density $n_0 \approx 0.7 \times 10^{20}/\text{cm}^3$ is close to the experimental value [12]. The self-compensation effect for $x \gg x^* \approx 0.5$ % is a characteristic signature of the CK state: on entering this state the Tl ions fluctuate

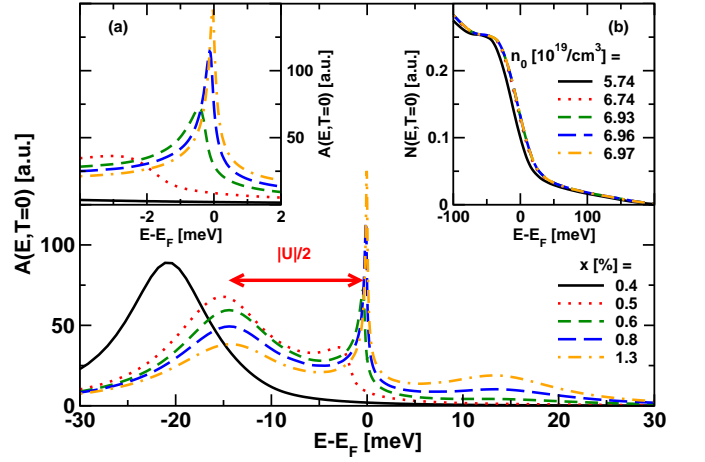


FIG. 2: (Color online) Tl spectral function $A(E, T = 0)$ versus $E - E_F$ for a range of Tl dopings x . Inset (a): region near $E = E_F$ showing the CK resonance. Inset (b): PbTe valence band density of states $N(E)$ versus $E - E_F$ for x as in the main panel [22] (legend: hole densities n_0 for each x).

between Tl^{1+} and Tl^{3+} so the average valence is Tl^{2+} , which corresponds to no additional electrons being accepted or donated. The CK state may be destroyed by lifting the degeneracy of the pseudospin states, i.e. in the language of the spin Kondo effect, by applying a “magnetic field”. A “magnetic field” in the CK effect corresponds to doping or shifting μ . This has been achieved by counterdoping with In ions [10], which act as donors. The Kondo anomalies, e.g. in the resistivity, were observed to vanish, providing further support to the CK picture. The self-compensation effect can be seen also in the pinning of the hole chemical potential μ for $x > x^*$, shown in Fig. 1a. For $x < x^*$, μ grows nonlinearly with x and rapidly approaches the value $\mu^* = 225$ meV for $x > x^*$, both at $T = 1.8$ K and at $T = 77$ K.

Figure 2 shows the Tl s -electron spectral function $A(E, T = 0)$ at zero temperature and different dopings x . For small doping, $x < x^*$, the hole chemical potential μ lies above μ^* within the shallow part of the valence band density of states $N(E)$ (see Fig. 2b), consequently the splitting $\delta(\mu) = 2(\mu - \mu^*)$, see Fig. 1a, is large. Such a large splitting acts like a large Zeeman splitting in the conventional positive U Anderson model and polarizes the spectral function so that its weight lies mostly below the Fermi level E_F [4]. For $x \geq x^*$, μ approaches μ^* and a CK effect develops. The spectral function develops a sharp asymmetric Kondo resonance close to, but below E_F (see Fig. 2a) and an upper Hubbard satellite peak appears above E_F . Early tunneling experiments for low dopings $x < 0.3$ % showed only one resonant level below E_F [13], whereas more recent tunneling experiments for $x > 0.6$ % show two “quasilocals” peaks [12], a narrow one of width 6 meV close to E_F and a broader one of width 12 meV at a nearly constant energy 13-15 meV

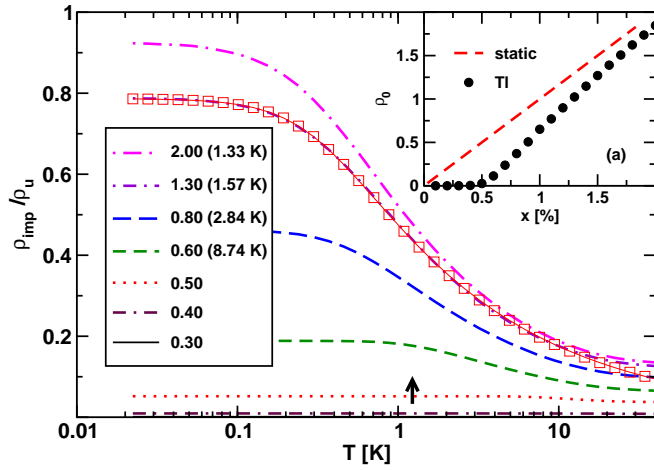


FIG. 3: (Color online) Impurity resistivity $\rho_{\text{imp}}(T)/\rho_u$ versus temperature T and a range of Tl concentrations x (in percent, legend: column 1). For $x > x^*$, ρ_{imp} is well described by the usual spin Kondo resistivity [23] (shown as open squares for $x = 1.3\%$), but with effective Kondo scales T_K^{eff} (legend: column 2). $\rho_u = 2n_{\text{Tl}}/(e^2\pi\hbar N_F^2\sigma_0)$ is the residual resistivity for unitary scatterers with $N_F = \mathcal{N}(\mu^*)$. The vertical arrow: $T_K = 1.23$ K. Inset (a): $\rho_0 = x\rho_{\text{imp}}(T=0)/\rho_u$ versus x (filled circles). Dashed line: ρ_0 for static unitary scatterers in place of Tl.

below this. Interpreting these as the Kondo resonance and the lower Hubbard satellite peaks in Fig. 2 yields $|U|/2 \approx 15$ meV and hence the value $U \approx -30$ meV used in our calculations. Since the CK resonance is temperature dependent [4], the above interpretation could be tested with temperature dependent studies of tunneling or high resolution photoemission spectra.

The temperature and doping dependence of the impurity resistivity, ρ_{imp} , is shown in Fig. 3. For $x < x^*$, Tl impurities act as acceptors with a well-defined valence state (Tl^{1+}). They therefore act as weak potential scatterers and consequently the resistivity is much below the unitary value, as seen in Fig. 3. For $x > x^*$, dynamic fluctuations between the nearly degenerate Tl^{1+} and Tl^{3+} states leads to the CK effect and ρ_{imp} approaches the resistivity for unitary scatterers at $T = 0$. For $x > x^*$, ρ_{imp} is well described by the *spin* Kondo resistivity [23] (open squares, Fig. 3) with a logarithmic form around $T \approx T_K^{\text{eff}}$, where T_K^{eff} is an effective Kondo scale, and T^2 Fermi liquid corrections at low $T \ll T_K^{\text{eff}}$, in qualitative agreement with experiment [6]. The effective Kondo scale T_K^{eff} is a function of the charge splitting $\delta(\mu)$ and T_K , and approaches the true Kondo scale T_K only asymptotically for $x \gg x^*$ (see legend to Fig. 3). Finally, Fig. 3a shows that the impurity residual resistivity is significant only when the CK effect is operative, i.e. for $x > x^*$, in qualitative agreement with experiment [6, 9].

Conclusions.— In summary, we investigated the normal state properties of $\text{Pb}_{1-x}\text{Tl}_x\text{Te}$ within a model of

Tl impurities acting as negative U centers. Our NRG calculations support the suggestion that the CK effect is realized in $\text{Pb}_{1-x}\text{Tl}_x\text{Te}$ [6, 7]. They explain a number of low temperature anomalies of $\text{Pb}_{1-x}\text{Tl}_x\text{Te}$, including the qualitatively different behavior below and above the critical concentration x^* , where $x^* \approx 0.5\%$ is close to $x_c \approx 0.3\%$ for the onset of superconductivity. At $x = x^*$, two nonmagnetic valence states of Tl become almost degenerate and the ensuing pseudospin CK effect results in a Kondo anomaly in the resistivity for $x > x^*$ and a residual resistivity approximately linear in x . Our results for these quantities and the carrier density $n_0(x)$ are in good qualitative agreement with experiments [6, 8, 9, 12]. For the Tl s -electron spectral function, we predict that one peak should be present far below E_F for $x < x^*$ and that a second temperature dependent Kondo resonance peak develops close to, but below E_F , on increasing x above x^* . This provides a new interpretation of measured tunneling spectra[12], which could be tested by temperature dependent studies of tunneling or photoemission spectra. In the future, it would be interesting to extend this work to include the effects of disorder within an Anderson-Hubbard model description.

We thank K. M. Seemann, D. J. Singh, H. Murakami, P. Coleman, G. Kotliar, and I. R. Fisher for discussions and D. J. Singh, H. Murakami and I. R. Fisher for data [8, 22]. V.Z. acknowledges support by Croatian MZOS Grant No.0035-0352843-2849, NSF Grant DMR-1006605 and Forschungszentrum Jülich. T. A. C. acknowledges supercomputer support from the John von Neumann Institute for Computing (Jülich).

-
- [1] S. A. Némov and Yu. I. Ravich, Phys. Usp. **41**, 735 (1998).
 - [2] B. A. Volkov, L. I. Ryabova, and D. R. Khokhlov, Phys. Usp. **45**, 819 (2002).
 - [3] A. Taraphder and P. Coleman, Phys. Rev. Lett. **66**, 2814 (1991).
 - [4] S. Andergassen, T. A. Costi, and V. Zlatić, Phys. Rev. B **84**, 241107(R) (2011).
 - [5] A. C. Hewson, *The Kondo Problem to Heavy Fermions*, Cambridge Studies in Magnetism (Cambridge University Press, Cambridge, U.K., 1997).
 - [6] Y. Matsushita, H. Bluhm, T. H. Geballe, and I. R. Fisher, Phys. Rev. Lett. **94**, 157002 (2005).
 - [7] M. Dzero and J. Schmalian, Phys. Rev. Lett. **94**, 157003 (2005).
 - [8] Y. Matsushita, P. A. Wianeci, A. T. Sommer, T. H. Geballe, and I. R. Fisher, Phys. Rev. B **74**, 134512 (2006).
 - [9] M. Matusiak, E. M. Tunncliffe, J. R. Cooper, Y. Matsushita, and I. R. Fisher, Phys. Rev. B **80**, 220403 (2009).
 - [10] A. S. Erickson, N. P. Breznay, E. A. Nowadnick, T. H. Geballe, and I. R. Fisher, Phys. Rev. B **81**, 134521 (2010).
 - [11] I. A. Chernik and S. N. Lykov, Sov. Phys. Solid State, **23**, 817 (1981).

- [12] H. Murakami, W. Hattori, Y. Mizomata, and R. Aoki, *Physica C* **273**, 41 (1996).
- [13] V. I. Kaidanov, S. A. Rykov, and M. A. Rykova, *Sov. Phys. Solid State* **31**, 1316 (1989)
- [14] P. W. Anderson, *Phys. Rev. Lett.* **34**, 953 (1975).
- [15] K. G. Wilson, *Rev. Mod. Phys.* **47**, 773 (1975); R. Bulla, T. A. Costi, and T. Pruschke, *Rev. Mod. Phys.* **80**, 395 (2008).
- [16] A. G. Mal'shukov, *Solid State Commun.* **77**, 57 (1991).
- [17] S. Ahmad, S. D. Mahanti, K. Hoang, and M. G. Kanatzidis, *Phys. Rev. B* **74**, 155205 (2006); K. Xiong, G. Lee, R. P. Gupta, W. Wang, B. E. Gnade, and K. Cho, *J. Phys. D: Appl. Phys.* **43**, 405403 (2010).
- [18] A. L. Shelankov, *Solid State Commun.* **62**, 327 (1987); I. Martin and P. Phillips, *Phys. Rev. B* **56**, 14650 (1997).
- [19] I. A. Drabkin and B. Ya. Moizhes, *Sov. Phys. Semicond.* **15**, 357 (1981).
- [20] K. Weiser, A. Klein, and M. Ainhorn, *Appl. Phys. Lett.* **34**, 607 (1979).
- [21] K. Nakayama, T. Sato, T. Takahashi, and H. Murakami, *Phys. Rev. Lett.* **100**, 227004 (2008).
- [22] D. J. Singh, *Phys. Rev. B* **81**, 195217 (2010).
- [23] T. A. Costi, A. C. Hewson, and V. Zlatić, *J. Phys.: Condens. Matter* **6**, 2519 (1994).
- [24] Upon using the lattice constant $a_0 = 6.46 \times 10^{-8}$ cm of the PbTe rocksalt structure.
- [25] G. Iche and A. Zawadowski, *Solid State Commun.* **10**, 1001 (1972); A. C. Hewson, J. Bauer, and W. Koller, *Phys. Rev. B* **73**, 045117 (2006).